


## $\gamma$ decay to the ground state from the excitations above the neutron threshold in the $^{208}\text{Pb}(p, p'\gamma)$ reaction at 85 MeV

B. Wasilewska,<sup>1</sup> M. Kmiecik <sup>1,\*</sup> M. Ciemała,<sup>1</sup> A. Maj,<sup>1</sup> F. C. L. Crespi,<sup>2,3</sup> A. Bracco,<sup>2,3</sup> M. N. Harakeh,<sup>4</sup> P. Bednarczyk,<sup>1</sup> S. Bottoni,<sup>2,3</sup> S. Brambilla,<sup>3</sup> F. Camera,<sup>2,3</sup> I. Ciepał,<sup>1</sup> N. Cieplicka-Oryńczak,<sup>1</sup> M. Csátos,<sup>5</sup> B. Fornal,<sup>1</sup> V. Gaudilla,<sup>6</sup> J. Grębosz,<sup>1</sup> J. Isaak,<sup>7</sup> Ł. W. Iskra,<sup>1,3</sup> M. Jeżabek,<sup>1</sup> A. J. Krasznahorkay,<sup>5</sup> S. Kihel,<sup>8</sup> M. Krzysiek,<sup>1</sup> P. Lasko,<sup>1</sup> S. Leoni,<sup>2,3</sup> M. Lewitowicz,<sup>9</sup> J. Łukasik,<sup>1</sup> M. Matejska-Minda,<sup>1</sup> K. Mazurek,<sup>1</sup> P. J. Napiorkowski,<sup>10</sup> W. Parol,<sup>1</sup> P. Pawłowski,<sup>1</sup> L. Q. Qi,<sup>11</sup> M. Saxena,<sup>10</sup> Ch. Schmitt,<sup>8</sup> Y. Sobolev,<sup>12</sup> B. Sowicki,<sup>1</sup> M. Stanoiu,<sup>13</sup> A. Tamii,<sup>14</sup> O. Wieland,<sup>3</sup> and M. Ziębliński<sup>1</sup>

<sup>1</sup>*Institute of Nuclear Physics Polish Academy of Sciences, PL-31342 Krakow, Poland*

<sup>2</sup>*Università degli Studi di Milano, I-20133 Milano, Italy*

<sup>3</sup>*INFN Sezione di Milano, I-20133 Milano, Italy*

<sup>4</sup>*Nuclear Energy Group, ESRIG, University of Groningen, Zernikelaan 25, 9747 AA Groningen, The Netherlands*

<sup>5</sup>*ATOMKI, Debrecen, Hungary*

<sup>6</sup>*Instituto de Física Corpuscular (IFIC), Valencia, Spain*

<sup>7</sup>*TU Darmstadt, Darmstadt, Germany*

<sup>8</sup>*IPHC, Strasbourg, France*

<sup>9</sup>*GANIL, CEA/DSAM and CNRS/IN2P3, CAEN Cedex 05, France*

<sup>10</sup>*Heavy Ion Laboratory, University of Warsaw, PL 02-093 Warsaw, Poland*

<sup>11</sup>*IPN, Orsay, France*

<sup>12</sup>*JINR, Dubna, Russia*

<sup>13</sup>*IFIN-HH, Bucharest, Romania*

<sup>14</sup>*RCNP, Osaka, Japan*



(Received 22 September 2021; accepted 24 December 2021; published 14 January 2022)

A new measurement of  $\gamma$  decay from the states above the neutron threshold in  $^{208}\text{Pb}$  has been performed at Cyclotron Centre Bronowice in Kraków, Poland. The main goal of the experiment was to observe the  $\gamma$  decay to the ground state from the isoscalar giant quadrupole resonance (ISGQR). To this day, the only published observation of this phenomenon dates back to the late 1980s, where  $\gamma$  decay to the ground state branching ratio was reported. At variance with the existing measurement using inelastic scattering of  $^{17}\text{O}$ , here proton inelastic scattering is employed. In particular, data were obtained for  $^{208}\text{Pb}(p, p'\gamma)$  at 85 MeV beam energy, where  $\gamma$  rays were measured for proton scattering angles  $8.9^\circ$ ,  $10.7^\circ$ ,  $12.5^\circ$ , and  $14.3^\circ$ . By applying a similar analysis method as in the previous experiment, the branching ratio of ISGQR gamma decay to the ground state was extracted from the data.

DOI: [10.1103/PhysRevC.105.014310](https://doi.org/10.1103/PhysRevC.105.014310)

### I. INTRODUCTION

Collective modes of excitation in the atomic nucleus have been extensively investigated for many years, giving an exclusive look into the bulk properties of this system. Especially, the measurement of the  $\gamma$  decay of the isovector giant dipole resonance (IVGDR) has proved to be a powerful tool to access information about the shape of the excited nucleus [1]. Moreover, it has been shown recently (see, e.g., Ref. [2]), that direct  $\gamma$  decay to low-lying states is a unique probe of the resonance wave function, and a testing ground for nuclear structure models. Although there were predictions showing that  $\gamma$  decay of the isoscalar giant quadrupole resonance (ISGQR) should also be sensitive to the deformation [3], so

far only one measurement of such a decay has been reported [4].

The reason for the lack of the experimental data is the difficulty of the measurement: the  $\gamma$  decay above the neutron threshold (in the case of  $^{208}\text{Pb}$   $S_n = 7.368$  MeV) is hindered by the competing channel of neutron emission. It is estimated that for the IVGDR decay the probability of  $\gamma$  emission (i.e., through decay to the ground state via  $E1$  transition) is of the order of  $10^{-2}$  [5]. In the case of ISGQR, which decays to the ground state (g.s.) via  $E2$  transition, the probability is expected to drop by two orders of magnitude.

In the only measurement of the ISGQR  $\gamma$  decay, the heavy-ion inelastic scattering reaction  $^{208}\text{Pb}(^{17}\text{O}, ^{17}\text{O}'\gamma)$  at the beam energy of 381 MeV was used. The scattered projectiles were detected by cooled Si telescopes, while emitted  $\gamma$  rays were measured by a  $4\pi$  NaI:Tl spectrometer. The data were collected in coincidence mode. With this setup, the obtained branching ratio was  $4 \pm 1 \times 10^{-4}$  for the ISGQR [4]. The goal

\*Corresponding author: [Maria.Kmiecik@ifj.edu.pl](mailto:Maria.Kmiecik@ifj.edu.pl)

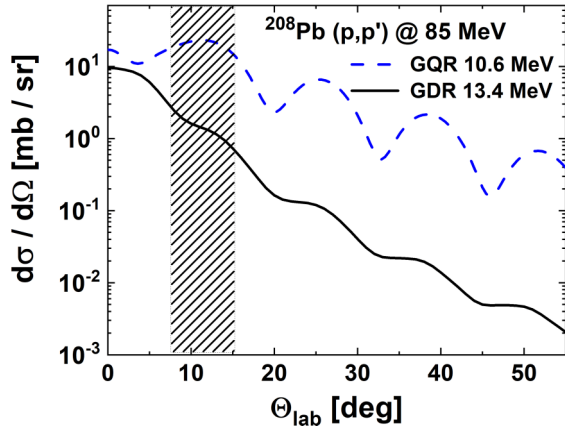


FIG. 1. Differential cross sections of ISGQR and IVGDR excitations populated in the inelastic scattering of the 85 MeV proton beam on  $^{208}\text{Pb}$ , calculated within the DWBA framework using the FRESKO code [10]. The angle range of the KRATTA modules (dashed grey area) is marked.

of the experiment reported here is to study the decay to the ground state from states excited in the ISGQR region in  $^{208}\text{Pb}$  using an alternative probe. In particular, we investigated proton inelastic scattering with an innovative setup implemented at the Cyclotron Centre Bronowice (CCB) facility in Kraków.

## II. EXPERIMENTAL SETUP

The experiment was performed at Cyclotron Centre Bronowice in Kraków, Poland, a facility dedicated mainly to the proton radiotherapy. The set-up consisted of eight large-volume  $\text{BaF}_2$   $\gamma$ -ray detectors of the HECTOR (High Energy detector) array [6], placed at 35 cm from the target, at  $\vartheta_H = 127^\circ$ , and 16 triple telescopes of the KRATTA (KRAKÓW Triple Telescope Array) array [7] for light charged particle identification and energy measurement. Fast plastic scintillators were placed in front of the KRATTA detectors, ensuring good time resolution. The prompt time peak between  $\gamma$  rays detected in  $\text{BaF}_2$  and protons detected in the plastic scintillators was estimated to have  $\sigma \approx 1.5$  ns. The KRATTA detectors were positioned 90 cm from the target, at four angles  $\vartheta_K = 8.9^\circ, 10.7^\circ, 12.5^\circ, 14.3^\circ$ , with four detectors for each angle, covering the location of the predicted second maxima of the differential cross sections for IVGDR and ISGQR excitations (see Fig. 1). As each detector had an opening of  $\Delta\vartheta = 1.8^\circ$ , the solid angle covered by the particle detectors was equal to 15 msr. The setup is described in more detail in Ref. [8].

In the experiment, an enriched (99.98% of  $^{208}\text{Pb}$ ), 48  $\mu\text{m}$  thick lead target was irradiated by an 85 MeV proton beam. The measurement was run in coincidence mode in which the data acquisition was triggered by a signal in at least one  $\gamma$ -ray detector and at least one fast plastic scintillator.

The obtained data were processed according to the procedure described in Ref. [9] and the analysis followed closely the one used in Ref. [4]. The DWBA (distorted-wave Born approximation) approach was employed using the FRESKO code [10] to calculate the differential proton elastic scattering

TABLE I. The parameters used within the FRESKO code to calculate the differential cross sections for the excitations in  $^{208}\text{Pb}$ .

| State   | Transition | Energy (MeV) | $B(E1 \uparrow)$ ( $e^2\text{fm}^2$ ) | DEF( $E1$ ) (fm) |
|---------|------------|--------------|---------------------------------------|------------------|
| $2_1^+$ | $E2$       | 4.1 [14]     | 2870 [14]                             | 0.38             |
| ISGQR   | $E2$       | 10.6 [4]     | 5350 [4]                              | 0.63             |
| IVGDR   | $E1$       | 13.4 [18]    | 60.9 [15]                             | n.a.             |

on  $^{208}\text{Pb}$  as well as the excitation cross section of the first  $2^+$  level, IVGDR, and ISGQR in  $^{208}\text{Pb}$ . The statistical decay of excited  $^{208}\text{Pb}$  to the ground state was calculated with the use of the ONE-STEP code [11], which is based on the Hauser-Feshbach formalism [12].

## III. PARAMETRIZATION OF THE THEORETICAL CALCULATIONS

In the DWBA calculations, the parameters of the optical potential are those of the empirical parametrization of Ref. [13], which was derived from the measurements in a wide range of nuclear masses and proton-beam energies. The used potential had a Woods-Saxon shape, with real and imaginary volume parts, and a spin-orbit part.

For the discrete  $2^+$  transition in  $^{208}\text{Pb}$ , the tabular values of reduced transition probability and deformation parameter [14] were used. In the case of the giant resonances, the problem was simplified to the collective excitation of the giant resonances at the corresponding centroid energies of the previously well-determined resonance shapes. The IVGDR energy-weighted sum rule (EWSR) was obtained from the  $B(E1)$  distribution measured in the  $(p, p')$  reaction at 295 MeV [15]. The total  $B(E1)$  value measured in this experiment was  $60.9 e^2\text{fm}^2$ , which corresponds to 111% EWSR for the IVGDR. Based on previous investigations it was assumed that the ISGQR exhausts 70% of the corresponding EWSR [4].

The nuclear part of the transition potential of the ISGQR was calculated following the formalism presented by Satchler [16,17]. It was treated within the standard collective model, where the excitation is described by the deformation of the optical potential. The deformation parameter  $\beta_l$  was calculated according to the formula given in Ref. [16]:

$$\beta_l = \left[ l(2l+1) \left( \frac{\hbar}{2mR^2} \frac{4\pi}{3AE} \right) \right]^{1/2}. \quad (1)$$

The deformation length [DEF( $E1$ )] was calculated as  $\text{DEF}(E1) = R\beta_l$  [10]. All used parameters are summarized in Table I.

For the sake of consistency, the calculations for the IVGDR were made with the FRESKO code, assuming Coulomb excitation dominates. The calculations were cross-checked with a modified version of the DWUCK4 code [19] to include IVGDR excitation, proving that the nuclear interaction plays a negligible role in the IVGDR excitation for the employed reaction.

The FRESKO calculations were tested using the literature values of the differential cross sections for the first  $2^+$  ex-

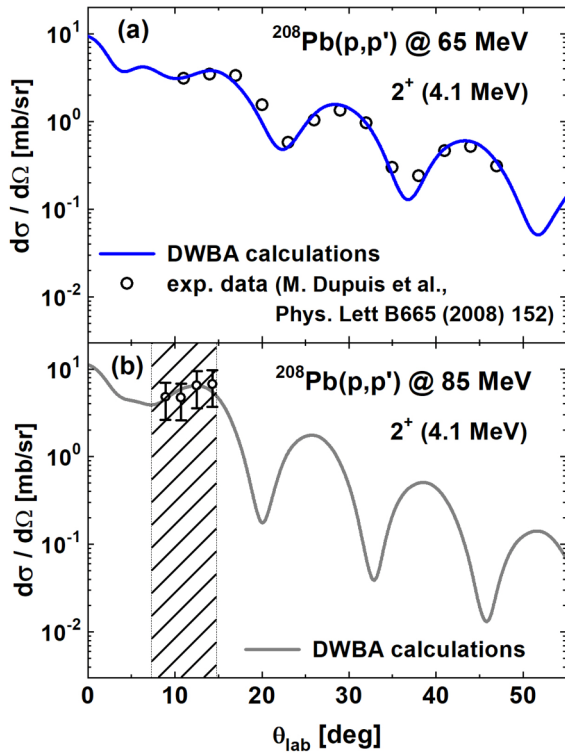


FIG. 2. Upper panel (a): comparison of the FRESKO calculated differential cross section (blue line) and the experimental results (black open circles) for  $2_1^+$  excitation in the  $^{208}\text{Pb}(p, p')$  reaction at 65 MeV [20]. Bottom panel (b): comparison of the calculated cross-section (grey line) and the present measurement of  $2_1^+$  excitation in the  $^{208}\text{Pb}(p, p')$  reaction at 85 MeV.

cited state of  $^{208}\text{Pb}$  obtained in the  $^{208}\text{Pb}(p, p')$  reaction at 65 MeV [20] [Fig. 2(a)]. Figure 2(b) shows the differential cross section measured for the  $2_1^+$  state in the present experiment and the DWBA calculations result for protons of 85 MeV energy. The excellent agreement between calculated and mea-

sured values at the two bombarding energies proves adequacy of the adopted calculation approach.

#### IV. EXTRACTION OF THE IVGDR AND ISGQR PROPERTIES

For each coincidence event, the excitation energy,  $E^*$ , of the nucleus was derived from the measured energy of the inelastically scattered proton. The events, in which only one proton and at least one  $\gamma$  ray were detected, were collected in  $E_\gamma$  vs  $E^*$  matrices. Depending on the measured time difference between a proton detection and the coincident  $\gamma$ -ray detection, the event was assigned either to the true coincidence [Fig. 3(a)] or the random coincidence matrix [Fig. 3(b)].

The main interest in this experiment was for the measurement of the  $\gamma$ -ray energy spectrum corresponding to the  $\gamma$  decay to the ground state. The spectrum was produced by setting on the matrices the condition  $|E_\gamma + 0.5 - E^*| \leq 1$  [MeV], represented by red lines in Fig. 3. In Fig. 4(a),  $\gamma$ -ray spectra corresponding to the g.s. gated decays for the true coincidence events (green triangles) and random coincidence events (blue dots) are presented. Figure 4(b) presents excitation energy spectra measured with the same conditions showing good correspondence to  $\gamma$ -ray spectra. In the analysis, an additional background originating from reactions on the Mylar foil covering the exit window of the scattering chamber was also taken into account (orange squares). It contains the events from the excitation and decay of  $^{12}\text{C}$ , necessary to be considered because of its high-energy part originating from 15.1 MeV excited states decay. The  $^{12}\text{C}$  background spectra were obtained using proton inelastic scattering on  $^{12}\text{C}$  target, and after normalization to the number of reactions at Mylar foil, employed as an experimental background. The resulting “true” experimental spectra, in which both random coincidences and other background sources were subtracted, are presented in Fig. 4 as open squares. In the  $\gamma$ -ray spectrum [Fig. 4(a)], the peaks recognized as transitions from the  $3_1^-$  (2.6 MeV) and  $2_1^+$  (4.1 MeV) excited states of  $^{208}\text{Pb}$  to the g.s. are evident. In the high-energy part of the

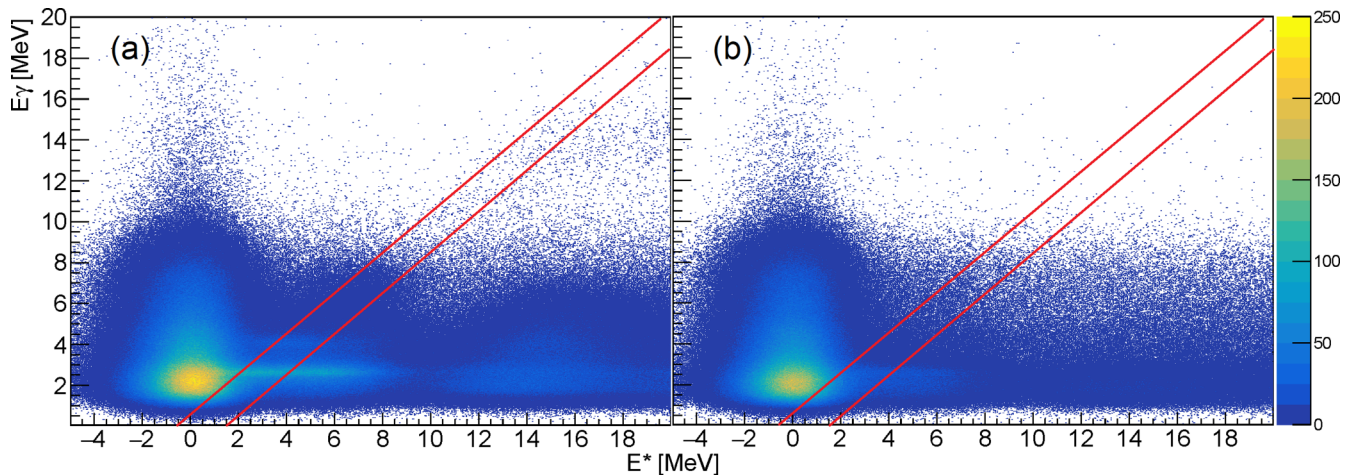


FIG. 3. The coincidence matrices of the  $^{208}\text{Pb}(p, p'\gamma)$  reaction at 85 MeV; true coincidence events (a) and random coincidence events (b). The gate applied to select those events which decay to the g.s. by emission of a single  $\gamma$  ray (having  $E_\gamma = E^*$ ) is marked by red lines.

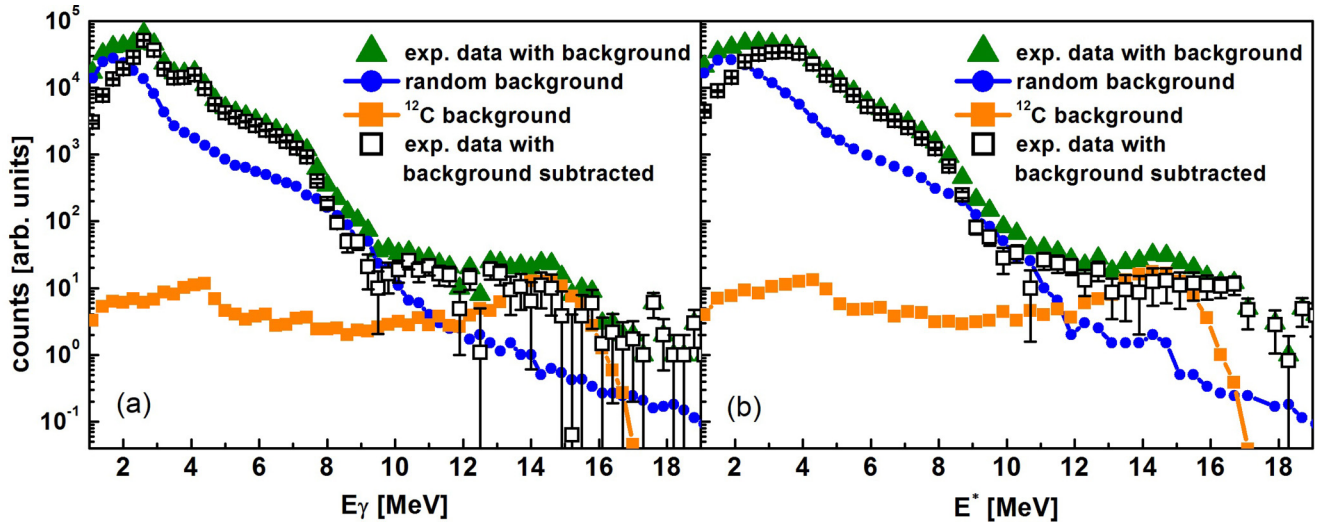


FIG. 4. Four  $\gamma$ -ray energy (a) and excitation energy (b) spectra: the spectrum corresponding to the “true + random” events of  $\gamma$  decay to the g.s. in  $^{208}\text{Pb}$  measured by HECTOR array (green triangles); the spectrum corresponding to “random” events (blue dots); the spectrum due to  $^{12}\text{C}$  background (orange squares); and finally the spectrum after subtraction of the “random” events and  $^{12}\text{C}$  background (open squares). The experimental background subtracted spectra show bumps corresponding to ISGQR (10–12 MeV) and to IVGDR (around 14 MeV). The increase in the  $^{12}\text{C}$  background spectra comes from 15.1 MeV state.

spectrum, structures in the regions of the expected  $\gamma$  decays to the g.s. (between 9 and 15 MeV) of the ISGQR and IVGDR are distinct. In the excitation energy spectrum [Fig. 4(b)] the high energy structures corresponding to giant resonances are visible, while  $3^-$  and  $2^+$  excitations are less pronounced because of the KRATTA energy resolution. The IVGDR and ISGQR features were obtained by analyzing the background subtracted  $\gamma$ -ray spectrum.

#### A. Analysis of the $\gamma$ decay from the IVGDR to the ground state

To study the decay of the ISGQR it was necessary to subtract the events due to the IVGDR  $\gamma$  decay to the ground state. To describe them, the multistep compound GR decay model (MSC) in the two-step approximation was adopted. In this approach, the cross section for the  $\gamma$  decay to the ground state can be described as [4]

$$\begin{aligned} \sigma_{p,p'\gamma_0}(E) &= \sigma_{p,p'}(E; B(EI) = 1) b_{EI}(E) \left[ \frac{\Gamma_{\gamma_0}}{\Gamma} + \frac{\Gamma^\downarrow}{\Gamma} B_{CN}(E) \right], \quad (2) \end{aligned}$$

where

- $\sigma_{p,p'}(E; B(EI) = 1)$  is the energy-dependent excitation cross section for a unit reduced transition probability;
- $b_{EI}(E)$  is the energy-dependent reduced transition probability for a given resonance;
- $\Gamma_{\gamma_0}$  is the direct  $\gamma$  decay width of the GR, calculated from the principle of detailed balance;
- $\Gamma^\downarrow$  is the spreading width of the GR;
- $\Gamma$  is the total width of the GR;
- $B_{CN}(E)$  is the energy-dependent compound nucleus branching ratio.

This equation provides a sum of two cross sections: the direct  $\gamma$  decay to the g.s. ( $\sigma_D$ ), and the compound nucleus

$\gamma$  decay to the g.s. ( $\sigma_{CN}$ ). These two contributions to the total (measured) cross section were determined separately as described below.

The unit cross section  $\sigma_{p,p'}(E; B(EI) = 1)$  was calculated with the use of the FRESKO code with the angular range covered in the experiment taken into account. The energy-dependent reduced transition probability [ $b_{EI}(E)$ ] for an IVGDR was obtained from the strength distribution measured in proton inelastic scattering at 295 MeV [15]. The compound nucleus branching ratio  $B_{CN}(E)$  was computed with the ONE-STEP program, a modified version of the CASCADE code [11]. The total width of the IVGDR was assumed as  $\Gamma = 3.9$  MeV [18], and the compound nucleus ratio as  $\Gamma^\downarrow/\Gamma = 1$  [21].  $\Gamma_{\gamma_0}$  was calculated following the formula [22]

$$\Gamma_{\gamma_0} = \frac{8\pi(l+1)}{l[(2l+1)!!]^2} \left[ \frac{E_\gamma}{\hbar c} \right]^{2l+1} \frac{2l+1}{2l'+1} B(EI, 0 \rightarrow n) \text{ [MeV]}, \quad (3)$$

where  $l$  and  $l'$  are spins of the ground state and the resonance, respectively.

The calculations were folded with the HECTOR response matrix, as well as the response of KRATTA detectors, and normalized to the detected number of counts for the decays from the  $2^+$  state measured in coincidence. This state decays by almost 100% via  $\gamma$  decay to the ground state; therefore, we assumed that the cross-sections for the  $^{208}\text{Pb}(p, p')$  and  $^{208}\text{Pb}(p, p'\gamma)$  reactions are equal. The normalization factor can be described by the following equation:

$$\xi_{2^+} = \frac{N_{2^+}}{\sigma_{2^+} \epsilon(E_{2^+})}, \quad (4)$$

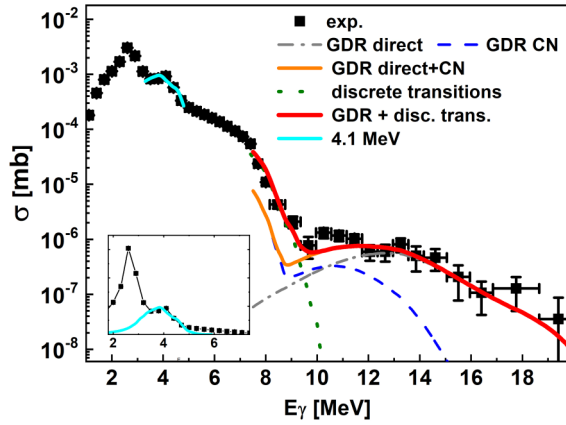


FIG. 5. The experimental energy spectrum presented in Fig. 4 with the calculated  $\gamma$ -ray energy spectra of the IVGDR  $\gamma$ -ray decay (orange solid line) and its components: direct decay (dash-dotted grey line) and compound decay (dashed blue line);  $\gamma$ -ray decay of the 7–10 MeV states (dotted green line). A sum spectrum of the IVGDR and discrete states in the 7–10 MeV region is also presented as a red line. Inset: The experimental  $\gamma$ -ray energy spectrum and the calculated one for the  $\gamma$ -ray decay to the g.s. of the  $^{208}\text{Pb}$  from the first  $2^+$  state (light blue line).

where

- $N_{2^+}$  is the number of detected  $\gamma$  decays from the  $2^+$  state to the g.s. in the experiment;
- $\epsilon(E_{2^+})$  is the detection efficiency of the HECTOR array for the  $2^+$  transition;
- $\sigma_{2^+}$  is the calculated cross section for the excitation of the  $2^+$  state in the  $^{208}\text{Pb}(p, p')$  reaction at 85 MeV.

In the inset of Fig. 5, the calculated  $\gamma$ -ray spectrum for the decay of first  $2^+$  state in  $^{208}\text{Pb}$  (light blue line) and the experimental data points after the aforementioned normalisation procedure are shown. Good agreement between experiment and theory is observed. In the calculated spectrum of the direct decay to the ground state the contributions of a few discrete states close to the neutron separation energy were taken into account. The two spin-flip excitations with spin  $1^-$  at 6.26 and 8.37 MeV were considered [23], along with three strong  $2^+$  states at 7.36, 8.86, and 9.34 MeV [24]. For each transition, an excitation cross section and the following  $\gamma$ -ray decay spectrum folded with the detector responses were calculated based on the given EWSR values [23,24]. The sum of decay of all considered transitions is presented in Fig. 5 as a green dotted line.

The resulting curves of the theoretical  $\gamma$ -ray energy spectra from the direct (dash-dotted grey line) and compound nucleus (dashed blue line) IVGDR decay to the g.s. are overlaid on the measured spectrum in Fig. 5. Their sum (orange line), as well as the curve with the added contributions coming from discrete states between 7 and 10 MeV (red line) cannot describe the excess of counts in the energy region between 10 and 12 MeV, where ISGQR  $\gamma$  decay is expected to be seen. It is discussed in the next section.

Using quantities described above, characterizing the IVGDR excitation and decay, we deduced the branching ratio

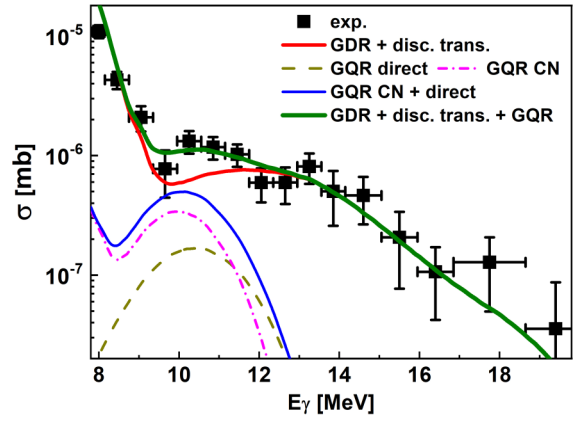


FIG. 6. Experimental energy spectrum presented in Fig. 4 with the calculated  $\gamma$ -ray energy spectra of the  $\gamma$  decay of the IVGDR together with 7–10 MeV states (red line); the ISGQR (calculated assuming 70% of ISGQR EWSR)  $\gamma$ -ray decay of the direct (dashed olive line) and compound (dash-dotted pink line) components; the sum of the  $\gamma$ -ray decay of the IVGDR, states between 7–10 MeV, and the ISGQR (dark green line). In the energy region of the ISGDR the calculations do not describe well the experimental data.

for the  $\gamma$ -ray decay to the ground state as

$$(\Gamma_{\gamma_0}/\Gamma)_{\text{GDR}} = \sum_E \frac{\sigma_{x,x'}\gamma_0(E)}{\sigma_{x,x'}(E)}. \quad (5)$$

The obtained branching ratio  $(\Gamma_{\gamma_0}/\Gamma)_{\text{GDR}} = 1.7 \times 10^{-2} \pm 0.5 \times 10^{-2}$  ( $\pm 0.3 \times 10^{-2}$  stat. and  $\pm 0.4 \times 10^{-2}$  syst.) is in perfect agreement with the literature value [5] of  $1.7 \times 10^{-2} \pm 0.2 \times 10^{-2}$ .

### B. Analysis of the ISGQR $\gamma$ -ray decay to the ground state

The computed  $\gamma$ -decay to the g.s. spectrum of the IVGDR and the discrete transitions (red line) along with calculations

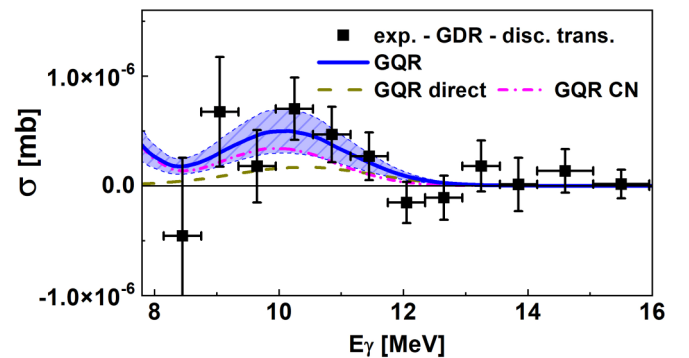


FIG. 7. Experimentally measured  $\gamma$ -ray energy spectrum fulfilling the ground-state decay condition after subtraction of the contribution from discrete states and from the IVGDR (black squares). The fitted direct (dashed olive line) and compound (dash-dotted pink line) components of the ISGQR  $\gamma$ -ray decay to the g.s. calculated spectra are presented as well. The summed energy spectrum for the ISGQR  $\gamma$ -ray decay to the g.s. (blue line) is also shown with uncertainty stemming from the normalization error.

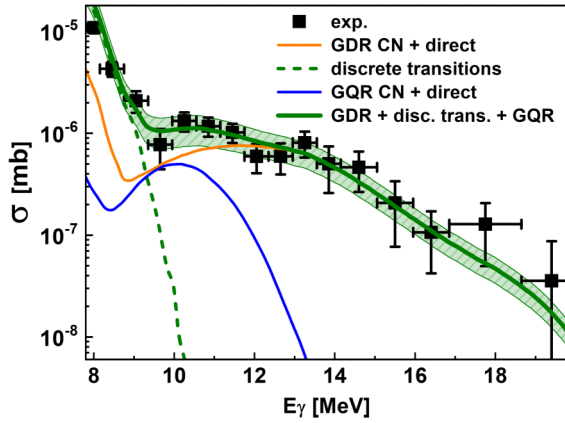


FIG. 8. The high energy part of the experimental  $\gamma$ -ray energy spectrum presented in Fig. 4 with the calculated theoretical  $\gamma$ -ray energy spectrum of the IVGDR  $\gamma$ -ray decay (orange line), the discrete states in the 7–10 MeV range (dashed green line), and the ISGQR (calculated assuming 112% of ISGQR EWSR)  $\gamma$ -ray decay (blue line). The calculated sum spectrum comprising the aforementioned transitions (green line) with the uncertainties stemming from the normalisation procedure (green shadow area) is also presented.

for the ISGQR direct (dashed olive line) and compound (dash-dotted pink line)  $\gamma$ -ray decays are presented in Fig. 6. In the calculations, the ISGQR width was assumed to be FWHM = 2.0 MeV [4] and 70% of the ISGQR EWSR was used. The resulting theoretical spectrum could not describe the observed excess of counts in the energy region of ISGQR in the experimental data (Fig. 6).

The  $(\Gamma_{\gamma_0}/\Gamma)_{\text{GQR}}$  branching ratio in the ISGQR energy region was obtained by fitting the experimental spectrum—after subtraction from the IVGDR component and the contribution from discrete states—in the region expected to be populated by the ISGQR (9.4–11.8 MeV). The result is displayed in Fig. 7. The  $\gamma$ -ray energy spectrum calculated using fitted ISGQR strength shows good agreement with the experimental data (see Fig. 8). The obtained, fitted ISGQR strength corresponds to  $112 \pm 32\%$  ( $\pm 25\%_{\text{stat.}}$  and  $\pm 20\%_{\text{syst.}}$ ) of the ISGQR EWSR. The resulted branching ratio for the  $\gamma$ -ray decay in the ISGQR energy region to the ground state  $(\Gamma_{\gamma_0}/\Gamma)_{\text{GQR}} = 3 \times 10^{-4} \pm 1 \times 10^{-4}$  ( $\pm 0.6 \times 10^{-4}_{\text{stat.}}$  and  $\pm 0.7 \times 10^{-4}_{\text{syst.}}$ ) is consistent within uncertainties with the value  $4 \times 10^{-4} \pm 1 \times 10^{-4}$  measured using the  $^{17}\text{O}$  inelastic scattering reaction [4]. The obtained branching ratio values for  $\gamma$  decay of giant resonances in  $^{208}\text{Pb}$  are summarized in Table II. Please note that the relatively large systematic errors of the  $\gamma$  decay branching ratio for both IVGDR and ISGQR come from uncertainties of the normalization of the calculated spectrum to the experimental  $2^+$  state.

## V. SUMMARY AND OUTLOOK

The  $\gamma$  decay of the ISGQR in  $^{208}\text{Pb}$  was studied with an innovative setup implemented at the CCB facility in Kraków, Poland. The data show, in line with the expectations, that giant resonances (ISGQR and IVGDR) were excited in the

TABLE II. Branching ratios for the  $\gamma$ -ray decay to the g.s. for the  $^{208}\text{Pb}$  IVGDR and ISGQR excitations.

|       | $(\Gamma_{\gamma_0}/\Gamma)_{\text{GR}}$                |
|-------|---------------------------------------------------------|
| IVGDR | $1.7 \times 10^{-2} \pm 0.5 \times 10^{-2}$ (this work) |
|       | $1.7 \times 10^{-2} \pm 0.2 \times 10^{-2}$ [5]         |
| ISGQR | $3 \times 10^{-4} \pm 1 \times 10^{-4}$ (this work)     |
|       | $4 \times 10^{-4} \pm 1 \times 10^{-4}$ [4]             |

$^{208}\text{Pb}(p, p')$  reaction at the beam energy 85 MeV and the decay to the ground state of both the ISGQR and the IVGDR was observed. Moreover, with use of a different probe (proton beam instead of  $^{17}\text{O}$  ions) and reaction energy, our extracted  $\gamma$ -ray decay branchings to the ground state for both ISGQR and IVGDR are in agreement with the previously published values [4,5]. In particular, the latter is in line with results of analysis by Beene *et al.* [25], showing a probability of ISGQR decay through the compound nucleus that is comparable to that by direct channel. The obtained result shows that  $^{208}\text{Pb}$  ISGQR  $\gamma$ -ray decay through the compound nucleus is of the same or even greater importance as direct decay. These features make testing the theoretical models [2] difficult with the studied case, but the obtained results show the feasibility for similar investigations in other nuclei. Testing the existing value of the  $\gamma$  decay branching ratio with another reaction would provide a solid base for future work using the same setup, addressing other nuclei where the direct component could become more important. To test the theory in the direct  $\gamma$  decay observable is experimentally very challenging, but it is very important to try to get as much detail as possible on the resonance wave functions.

To provide more details on the ISGQR  $\gamma$ -ray decay, a subsequent experiment with an improved setup is planned. The energy resolution of the inelastically scattered protons measurement will be enhanced by placing the detectors inside a vacuum chamber. The number of measured proton scattering angles will be increased, enabling the MDA (multipole-decomposition analysis) technique [15,26]. The  $\gamma$ -ray detectors will be replaced with new-generation scintillators, such as the PARIS clusters [27] or large  $\text{LaBr}_3:\text{Ce}$  detectors [28], improving the energy resolution of the  $\gamma$ -ray energy spectra. Additionally, the  $\gamma$ -ray detectors will be positioned at the angles  $\vartheta = 45^\circ, 90^\circ$ , and  $135^\circ$ , facilitating the discrimination between  $E1$  and  $E2$  transitions.

The present finding, in line with the existing work based on the use of another excitation reaction, provides support for carrying out in the future other studies of  $\gamma$ -ray decay from giant resonances in several nuclei and using improved experimental conditions. Such results are expected to test predictions in a detailed way.

## ACKNOWLEDGMENTS

The project has received funding from the European Union's Horizon 2020 Research and Innovation Programme under Grant Agreements No. 654002 (ENSAR2 project) and No. 730989 (IDEAAL project). It was also supported

by Polish National Science Centre Grants No. 2015/17/N/ST2/04034 and No. 2015/17/B/ST2/01534, the Hungarian NKFI/OTKA Foundation Grant No. K124810,

and the COPIN-IN2P3 and COPIGAL collaborations between Poland and France. The excellent work of the CCB cyclotron team is appreciated.

- 
- [1] P. F. Bortignon, A. Bracco, and R. A. Broglia, *Giant Resonances* (Harwood Academic, London, 1998).
- [2] W. L. Lv, Y. F. Niu, and G. Colò, *Phys. Rev. C* **103**, 064321 (2021).
- [3] M. N. Harakeh and A. van der Woude, *Giant Resonances* (Oxford University Press, Oxford, 2001).
- [4] J. R. Beene, F. E. Bertrand, M. L. Halbert, R. L. Auble, D. C. Hensley, D. J. Horen, R. L. Robinson, R. O. Sayer, and T. P. Sjoreen, *Phys. Rev. C* **39**, 1307 (1989).
- [5] J. R. Beene, R. L. Varner, and F. E. Bertrand, *Nucl. Phys. A* **482**, 407 (1988).
- [6] A. Maj *et al.*, *Nucl. Phys. A* **571**, 185 (1994).
- [7] J. Łukasik *et al.*, *Nucl. Instrum. Methods Phys. Res., Sect. A* **709**, 120 (2013).
- [8] B. Wasilewska *et al.*, *Acta Phys. Pol. B* **50**, 469 (2019).
- [9] B. Wasilewska *et al.*, *Acta Phys. Pol. B* **48**, 415 (2017).
- [10] I. J. Thompson, Fresco code, <http://www.fresco.org.uk>, accessed on 17 September 2021.
- [11] F. Pühlhofer, *Nucl. Phys. A* **280**, 267 (1977); A. Bracco, CASCADE code, modified version.
- [12] W. Hauser and H. Feshbach, *Phys. Rev.* **87**, 366 (1952).
- [13] A. Nadasen, P. Schwandt, P. P. Singh, W. W. Jacobs, A. D. Bacher, P. T. Debevec, M. D. Kaitchuck, and J. T. Meek, *Phys. Rev. C* **23**, 1023 (1981).
- [14] B. Pritychenko, M. Birch, B. Singh, and M. Horoi, *At. Data Nucl. Data Tables* **107**, 1 (2016).
- [15] A. Tamii, I. Poltoratska, P. von Neumann-Cosel, Y. Fujita, T. Adachi, C. A. Bertulani, J. Carter, M. Dozono, H. Fujita, K. Fujita, K. Hatanaka, D. Ishikawa, M. Itoh, T. Kawabata, Y. Kalmykov, A. M. Krumbholz, E. Litvinova, H. Matsubara, K. Nakanishi, R. Neveling *et al.*, *Phys. Rev. Lett.* **107**, 062502 (2011).
- [16] G. R. Satchler, *Nucl. Phys. A* **195**, 1 (1972).
- [17] G. R. Satchler, *Nucl. Phys. A* **472**, 215 (1987).
- [18] A. V. Varlamov, V. V. Varlamov, D. S. Rudenko, and M. E. Stepanov, *Atlas of Giant Dipole Resonances, Parameters and Graphs of Photonuclear Reaction Cross Sections* (INDC, Vienna, 1999).
- [19] P. D. Kunz, program DWUCK (unpublished); M. N. Harakeh, modified version.
- [20] M. Dupuis *et al.*, *Phys. Lett. B* **665**, 152 (2008).
- [21] J. R. Beene, F. E. Bertrand, D. J. Horen, R. L. Auble, B. L. Burks, J. GomezdelCampo, M. L. Halbert, R. O. Sayer, W. Mittag, Y. Schutz, J. Barrette, N. Alamanos, F. Auger, B. Fernandez, A. Gillibert, B. Haas, and J. P. Vivien, *Phys. Rev. C* **41**, 920 (1990).
- [22] A. Bohr and B. R. Mottleson, *Nuclear Structure, Vol. II* (Benjamin, Reading, MA, 1975).
- [23] H. P. Morsch, P. Decowski, and W. Benenson, *Nucl. Phys. A* **297**, 317 (1978).
- [24] F. E. Bertrand, E. E. Gross, D. J. Horen, R. O. Sayer, T. P. Sjoreen, D. K. McDaniels, J. Lisantti, J. R. Tinsley, L. W. Swenson, J. B. McClelland, T. A. Carey, K. Jones, and S. J. Seestrom-Morris, *Phys. Rev. C* **34**, 45 (1986).
- [25] J. R. Beene, G. F. Bertsh, P. F. Bortignon, and R. A. Broglia, *Phys. Lett. B* **164**, 19 (1985).
- [26] I. Poltoratska, P. von Neumann-Cosel, A. Tamii, T. Adachi, C. A. Bertulani, J. Carter, M. Dozono, H. Fujita, K. Fujita, Y. Fujita, K. Hatanaka, M. Itoh, T. Kawabata, Y. Kalmykov, A. M. Krumbholz, E. Litvinova, H. Matsubara, K. Nakanishi, R. Neveling, H. Okamura *et al.*, *Phys. Rev. C* **85**, 041304(R) (2012).
- [27] A. Maj *et al.*, *Acta Phys. Pol. B* **40**, 565 (2009).
- [28] A. Giaz *et al.*, *Nucl. Instrum. Methods Phys. Res., Sect. A* **729**, 910 (2013).